



Optimal design of radial tire section layout based on thermal fatigue life improving

Kun Xing^a, Peng Cheng^a, Qingchun Wang^{a,*}, Haotian Li^b

^a School of Technology, Beijing Forestry University, No. 35 Qinghua East Road, Haidian District, Beijing 100083, China

^b Qingdao Haitong Axle Co., Ltd., No. 106, Jiefang Second Road, Jimo District, Qingdao, Shandong 266000, China

ARTICLE INFO

Keywords:

Tire
Thermal fatigue
Experimental design
Approximate model
Optimal design

ABSTRACT

The design of tire fatigue life was optimized by combining approximate model and finite element simulation, and compared with the tire endurance test results. The design variables are selected through sensitivity analysis of materials in various regions of the tire, and the thermal fatigue life of the tire is used as the objective function, and the approximate relationship between the design variables and the objective function is fitted based on the approximate model method, and the approximate model is optimized using genetic algorithm to find the optimal solution. The fatigue life of the tire is improved by about 25 %.

1. Introduction

With the rapid increase in car ownership, people's requirements for car safety are getting higher and higher. In the driving process, the acceleration, deceleration and steering of the car can be realized through the friction between the tires and the ground, so the driving performance of the car is closely related to the performance of the tire. The "burst" phenomenon caused by excessive tire temperature and fatigue damage is a common safety problem for automobiles, it can be seen that the durability and service life of tires has become the most concerned about the tire performance. Therefore, how to improve tire durability and service life from the design and manufacturing process has become an urgent problem for tire companies to solve, and The research on relevant issues is of great significance in today's rapid development of the automobile industry [1].

In recent years, radial tires have gradually replaced bias tires and become the standard tire for most cars [2]. Compared with bias tires, radial tires have good adhesion, low rolling resistance, strong cushioning, strong heat dissipation, fuel efficiency and durability. Therefore, the research related to radial tires is also the focus of attention in the tire industry today.

During the driving process of the vehicle, the tire is subjected to a variety of external forces, and its grounding area is deformed greatly and thus generates a large stress-strain, and the tire produces high-frequency stress-strain changes inside the tire with the high-speed rotation, which is the main reason for the tire fatigue damage [3]. In addition, due to the hysteresis effect of the rubber material and the periodic deformation of the tire during rolling, part of the kinetic energy inside the tire is converted into thermal energy to increase the internal temperature of the tire, and the temperature rise will accelerate the aging of the rubber material, which in turn accelerates the rate of tire fatigue damage. So, the fatigue damage of tires under the effect of heat is an important reason affecting the service life of tires and automobile safety. Therefore, the improvement of tire fatigue life by optimizing tire structure and improving material formulation has been a key concern in the tire industry and related research fields.

* Corresponding author.

E-mail address: wangqingchun@bjfu.edu.cn (Q. Wang).

The complex internal structure of tires, the variety of materials and uneven distribution, in addition to the tire analysis to multiple nonlinear problems, which caused great difficulties for the tire structure improvement and optimization design work. At present, the improvement of tire structure and performance optimization are mostly done by using finite element simulation technology to design parameters for a certain area of the tire, and by continuously trying to change certain parameters to achieve the purpose of improving the structure and optimizing the performance, this method mostly requires multiple design solutions verification and iterative process. Wang Guolin performed sensitivity analysis on six rubber materials near the bead area of a load radial tire, using the model parameters C_{10} of each materials design variables, to study the influence of material parameters on the variable energy density SENER, and a design solution for the combination of material parameters with better fatigue life performance was proposed [4]. Jiaojiao Yang addressed the fatigue damage problem in the bead area of radial tires, and effectively improved the fatigue damage phenomenon of the bead by increasing the height of the reverse wrapping of the tire casing cord, and ameliorated the fatigue life of the bead area of 175/70R14 semi-steel radial tires, and conducted tests to verify the improvement measures [5]. By optimizing the 0° belt layer structure of the load radial tire, Ye Jialei significantly reduced the deformation of the belt layer and the expansion rate of the outer diameter, which slowed down the fatigue damage phenomenon and thus improved the fatigue durability of the tire [6]. However, the accuracy of the finite element simulation results largely depends on the accuracy of the finite element model. A high-precision finite element model is bound to lead to a significant increase in the analysis and calculation time and cost. For engineering optimization problems, it is often necessary to carry out multiple analysis iterations, and the computing time of the computer will increase exponentially in this process. Therefore, for large-scale engineering optimization problems, it is difficult to complete only using finite element simulation technology [7].

In order to reduce the amount of computation and save the cost of trial time, Kleijnen proposed the concept of approximate modeling, using approximate models instead of computer programs in the product design process [8]. This method replaces the complex finite element model by constructing an approximate model, and the complex and time-consuming finite element simulation process by solving the approximate model, which simplifies the calculation process and ensures the accuracy of the calculation results. In fact, it uses various mathematical approximation methods to curve fit or interpolate a certain number of discrete points to predict more unknown points. With the development and maturity of the approximate modeling technique, it was widely applied to the optimization design process in various disciplines, and some scholars have applied the approximate modeling technique to the optimization design problem of tires. Lee designs the tire profile through an approximate model [9]. D. Meng used alternative models to alleviate the computational burden of multidisciplinary design and optimization problems based on uncertainty, established a smooth response surface for turbine blade performance, and solved a turbine blade design optimization problem [10]. Yan wei applied response surface methodology to optimize the thermal performance of microchannel in electric vehicle battery [28]. Li YQ optimizes the design of tires in terms of both grip and durability performance of 205/55R16 tires, and studies the influence of crown parameters on these two aspects of performance. The four tire parameters with the greatest influence on the grip and durability of the tire were selected as design variables from multiple crown parameters by using SPSS statistical software, and the mathematical models between the grip and durability and the four parameters were established separately by using Design-Expert software, and the approximate models were established by using the response surface method, and the four tire parameters were selected by using the relevant optimization algorithms. The optimized design of the tires has obtained a certain degree of performance improvement in terms of grip and durability [11]. Most of the tire optimization design studies are related to the tire structure, and the few studies that consider the influence of materials on tire fatigue performance only analyze a certain rubber material, and few studies consider multiple rubber materials at the same time to optimize the design of tire fatigue life.

This paper takes a load radial tire provided as the research object, establishes a tire finite element model and conducts temperature field and free rolling simulation; based on the results of temperature field and free rolling analysis, the tire fatigue life is calculated jointly using Fe-safe software, and the simulation calculation results are compared with the experimental results to verify the accuracy of the finite element model and analysis process; taking the tire thermal sensitivity analysis of the rubber material in each area of the tire cross-section is carried out with the tire thermal fatigue life as the consideration index, and the key research area is selected; the tire thermal fatigue life is taken as the objective function, the elastic modulus of each rubber material in the key area and the angle of the belt cord are the design variables, and the approximate relationship between the objective function and the design variables are fitted, and a suitable algorithm is applied to find the optimal solution of the objective function, and then the tire fatigue life in the design space is obtained. The optimal design solution for the tire fatigue life in the design space is then obtained.

2. Methods

2.1. Tire thermal fatigue life simulation analysis

2.1.1. Numerical model

Based on the 2D CAD drawing of the tire, the 2D finite element model of the tire is established to simulate the assembly and inflation conditions of the tire. The rubber element selected for the two-dimensional tire model are CGAX3H and CGAX4H, and the cord element is SFMGAXL. Yeoh model is selected as the constitutive model of rubber in this paper. It is a special form of reduced polynomial when $N = 3$. Its formula is:

$$W = C_{10}(I_1 - 3) + C_{20}(I_1 - 3)^2 + C_{30}(I_1 - 3)^3 \quad (1)$$

Where, W is the strain energy density, C_{10} , C_{20} and C_{30} are the constitutive parameters, I_1 is the deformation tensor invariant. The

model can well fit the mechanical properties of rubber under large deformation. The model parameters are obtained from the rubber tensile test. Through measuring the stress-strain data, the coefficients of the Yeoh model are fitted to obtain the model parameters of the rubber material. The model parameters of rubber materials are shown in Table 1.

There are three main mechanical performance parameters of tire skeleton material, namely, elastic modulus, Poisson's ratio and density. In addition, skeleton structure parameters need to be defined in tire finite element simulation, including cord angle, cord cross-sectional area, adjacent cord spacing and relative center plane position. Among them, the density and Poisson's ratio are provided by the tire manufacturer, and the elastic modulus is obtained through uniaxial tensile test. Mechanical performance parameters of each material in the skeleton structure are shown in Table 2.

The 3D model of the tire is obtained by rotating the 2D model around the central axis, the rubber elements selected for the 3D model of the tire were C3D6H and C3D8H, and the cord elements were SFM3D4R. The 3D analysis simulates the tire durability test conditions in a laboratory environment [12]. In order to shorten the time required for the durability test, an intensive experiment is adopted, the experimental loading conditions are set to 200 % of the maximum rated load, and the internal pressure of the tire is set to 80 % of the maximum rated air pressure. The specific parameter settings for tire durability experiments are shown in Table 3.

The statics analysis and calculation results of tire grounding conditions are shown in Fig. 1.

The process of 3D analysis is first the static analysis of the grounding condition, which simulates the process that the whole tire and the drum have never contacted. After that, the simulation analysis of tire braking and driving conditions is carried out, and the speed curve of tire rolling process is obtained to solve the angular velocity of tire free rolling. Finally, the simulation and analysis of the free rolling condition of the tire are carried out to simulate the experimental condition, and the stress, strain and volume information of the rubber element under the free rolling condition are obtained. The finite element simulation results of tire free rolling conditions are shown in Fig. 2.

2.1.2. Tire temperature field simulation analysis

Tire temperature field analysis is to simulate the temperature distribution in each region of the tire under free-rolling conditions, with the purpose of providing temperature data for experiments on fatigue performance parameters of the rubber material in each region of the tire [13] (see Fig. 3). When the tire is in the steady state rolling condition, the tire heat generation and heat dissipation reach equilibrium, at this time the tire temperature field no longer changes, because the tire circumferential temperature difference is ignored, so the temperature field distribution of the radial section of the tire can be regarded as the temperature field distribution of the whole tire. Based on the above analysis, this paper adopts the two-dimensional cross-sectional finite element model of the tire for temperature field analysis. Since the fatigue failure of tire occurs in the rubber structure, and the skeleton structure will not be damaged in advance, only the influence of the temperature field of the rubber structure on the fatigue life of the whole tire is considered in the tire temperature field analysis. Based on the above reasons, the two-dimensional tire mesh model used in tire temperature field analysis needs to remove the skeleton structure mesh.

Due to the effect of periodic stress during tire rolling, the hysteresis energy loss of rubber material in tire in one cycle can be expressed as:

$$E_l = V \int_c \sigma(t) d\varepsilon = \pi \cdot V \cdot \sigma_0 \cdot \varepsilon_0 \cdot \sin \delta \quad (2)$$

Where, V is the material volume, σ_0 is the stress amplitude, ε_0 is the strain amplitude, and δ is the hysteresis loss angle. The hysteresis loss angle of the tire rubber material are obtained from the thermal experiments.

However, during the actual rolling process of the tire, the periodic stress-strain curve it is subjected to is not a standard sine curve, but a periodic pulse form. For the actual stress-strain curve, it can be seen as the superposition of multiple sine waves with different phases and different amplitudes, which can be processed by Fourier transform and considering the hysteresis loss angle [14]:

$$E_L = \sum_{n=1}^N [\pi \cdot n \cdot V \cdot A_n^\sigma \cdot A_n^\varepsilon \cdot \sin(\varphi_n^\sigma - \varphi_n^\varepsilon + \delta_n)] \quad (3)$$

Where, n is Fourier series.

Table 1
Constitutive parameters of rubber materials.

Material name	Corresponding region	C_{10}	C_{20}	C_{30}
Q134	tread	0.56890	-6.953E-02	1.35238
Q210	side	7.244E-02	0.11048	-1.488E-02
Q315	wear	0.80833	-0.12632	2.499E-02
Q410	down	0.19877	0.24324	-2.509E-02
Q420	up	0.10751	0.10441	-1.324E-02
Q533	shoulder	0.49982	-5.403E-02	1.135E-02
Q710	bead	0.24787	0.11685	-9.701E-03
Q833	belt	0.12138	0.15886	-1.27E-02
Q870	carcass	0.45616	-1.8E-02	1.296E-02
Q910	inner	3.825E-02	6.151E-02	-8.029E-03

Table 2
Mechanical properties parameters of each material in the skeleton structure.

Skeleton structure	Elastic modulus (MPa)	Poisson's ratio	Density (kg/m ³)
bead	210,000	0.3	7800
carcass	166,463	0.3	7800
nylon	2826.2	0.4	1150
0#belt	122,151	0.3	7800
1#belt	164,981	0.3	7800
2#belt	164,983	0.3	7800
3#belt	127,032	0.3	7800

Table 3
Parameter setting table of tire 3D analysis.

Parameter	Value
Drum diameter	1707 mm
Drum width	800 mm
Tire center height	570 mm
frictional coefficient	0.2
Tire internal pressure	0.65 MPa
Roll up distance	7 mm
Load	75 kN

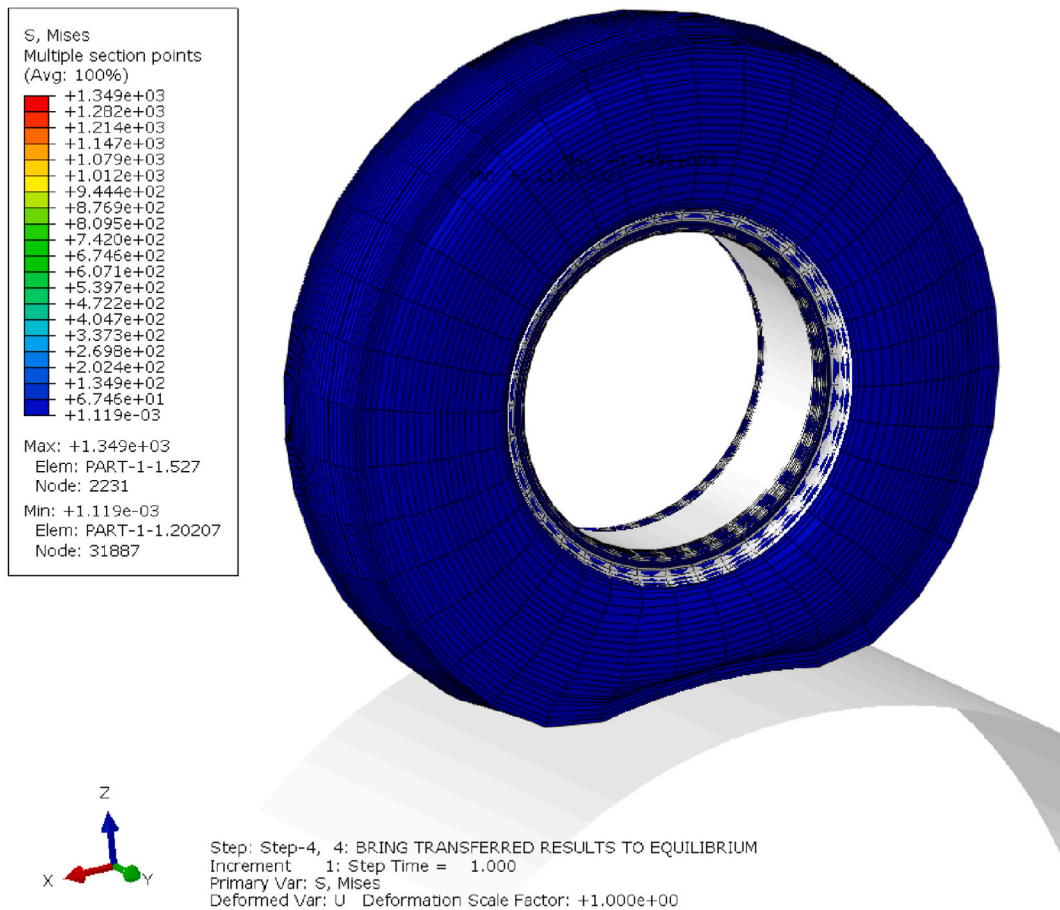


Fig. 1. Simulation results of tire grounding conditions.

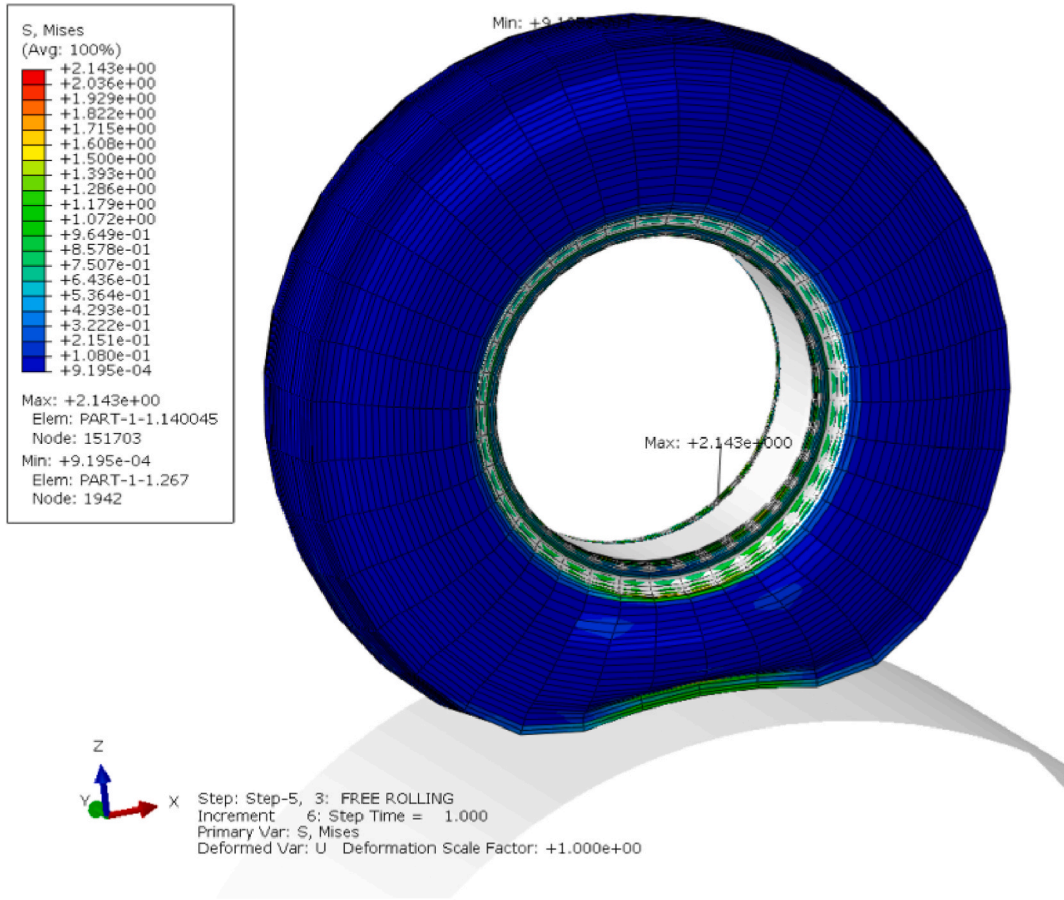


Fig. 2. Cloud diagram of simulation results for tire free rolling condition.

The tire temperature field analysis is based on the two-dimensional cross-section mesh model of the tire. For the element in the three-dimensional model of the tire, the stress and strain curve of the element in which the tire rolls for one cycle is the circumferential stress and strain curve of the corresponding element in the two-dimensional mesh model within one cycle, and the hysteresis energy loss of a single element is:

$$E_l = \sum_{d=1}^6 \sum_{n=1}^N [\pi \cdot n \cdot V \cdot A_n^\sigma \cdot A_n^\epsilon \cdot \sin(\varphi_n^\sigma - \varphi_n^\epsilon + \delta_n)] \tag{4}$$

Where, d is the component direction of stress and strain.

The heat generation rate of the rubber element is calculated from the thermal performance parameters of the rubber and the stress, strain and volume information of the rubber element in the free rolling condition. The calculation formula of heat generation rate of rubber unit is:

$$Q = \frac{E_l/V_e}{T_0} \tag{5}$$

Where, E_l is the lag energy loss of the unit, V_e is the unit volume, and T_0 is the tire rolling cycle.

Thermal performance parameters of each rubber material are shown in Table 4.

The heat generation rate is imported into the temperature field analysis model, and the convective heat transfer coefficient, heat flow temperature and the ambient temperature around the tire are set. Thermal boundary settings for each surface of the tire are shown in Table 5.

The temperature field analysis results are calculated as follows.

According to the analysis results, the highest temperature area in the tire under free rolling conditions is located in the up rubber section, with a maximum temperature of 108.3 °C. The second highest temperature area is located in the shoulder section of the tire, with a temperature of around 83 °C; The area with the lowest temperature is located in the side section, with a temperature of only about 30 °C. This is because the small cross-sectional width of the side section provides good heat dissipation conditions, resulting in

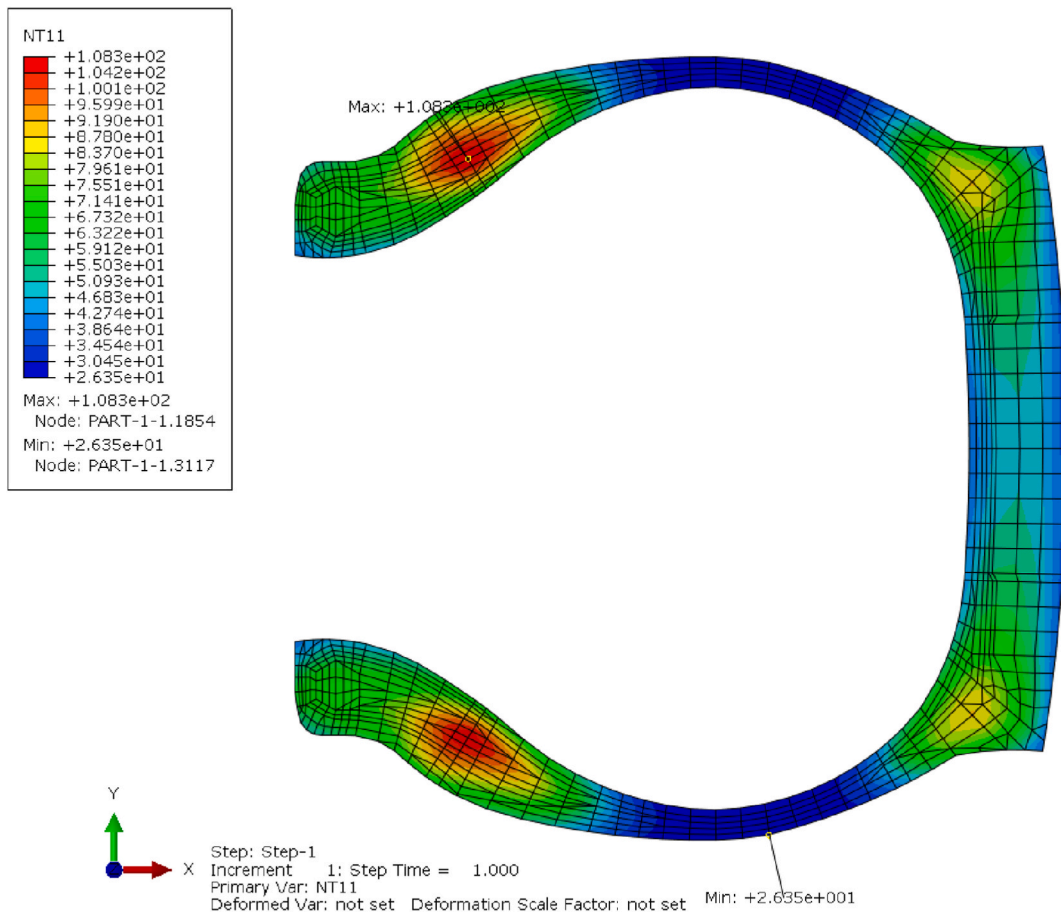


Fig. 3. Analysis results of tire temperature field.

Table 4
Thermal performance parameters of each rubber material.

Material name	Corresponding region	Thermal conductivity $W/(m \cdot K)$	Specific heat $J/(kg \cdot K)$	Density g/cm^3	Loss factor
Q134	tread	0.235	1.591	1.125	0.242
Q210	side	0.243	1.452	1.103	0.293
Q315	wear	0.277	1.590	1.165	0.174
Q410	down	0.264	1.376	1.151	0.288
Q420	up	0.214	1.355	1.103	0.263
Q533	shoulder	0.224	1.431	1.125	0.271
Q710	bead	0.221	1.085	1.124	0.367
Q833	belt	0.228	1.063	1.155	0.242
Q870	carcass	0.219	1.285	1.164	0.035
Q910	inner	0.220	1.442	1.207	0.265

Table 5
Thermal boundary settings for each surface of the tire.

Surface	Convective heat transfer coefficient ($W/m^2 \cdot C$)
Tread	38.3
Inner and bead	15.32
Side	22.98

the lowest temperature.

2.1.3. Tire thermal fatigue life simulation analysis

The precondition for the application of the crack growth method is that the specimen itself has defects or cracks, and the initial crack of the specimen gradually expands under the action of cyclic load, resulting in fatigue failure. The research shows that the energy release rate is the only factor that determines the crack growth rate in the crack growth process of rubber materials [15], and the energy release rate is the energy released by the expansion of unit area crack material, also known as material tear energy.

Based on the maximum tear energy theory, the thermal fatigue life of tire under free rolling condition is analyzed by finite element software. Lake and Lindley proposed a four-stage crack growth model (Lake-Lindley model) by studying the maximum tear energy and crack growth rate of rubber materials in the crack growth stage and fitting the relationship between them [17]. The model expression is shown in Eq. (6):

$$\begin{cases} \frac{da}{dN} = r_0, (T_{\max} < T_0) \\ \frac{da}{dN} = A(T_{\max} - T_0) + r_0, (T_0 \leq T_{\max} < T_t) \\ \frac{da}{dN} = BT_{\max}^F, (T_t \leq T_{\max} < T_c) \\ \frac{da}{dN} = \infty, (T_{\max} = T_c) \end{cases} \quad (6)$$

Where, r_0 is the crack growth rate at $T_{\max} < T_0$, T_0 is the threshold tear energy, T_t is the turning tear energy, T_c is the breaking tear energy, and A, B, F are constants related to the material. When the maximum tearing energy is greater than T_c , the crack will undergo unstable propagation [16]. In fact, the crack growth of rubber materials is mostly in the third stage - power law stage, so the crack growth in this stage can be approximately replaced by the whole crack growth process [17,18].

Take the logarithm of both sides of the third-stage formula of Lake-Lindley fatigue model to obtain:

$$\lg\left(\frac{da}{dN}\right) = \lg B + F \lg T_{\max} \quad (7)$$

In the third stage, the model curve is a straight line in the logarithmic coordinate system, and the slope of the straight line is the rubber material constant F .

The calculation formula of maximum tear energy is:

$$T_{\max} = 2f(\lambda)lE_0 \quad (8)$$

In the formula, E_0 is the strain energy density of the crack-free rubber specimen, which is obtained by simulation using the finite element software, l is the crack length set in advance, $f(\lambda)$ is a function related to strain, and can be expressed as Eq. (9):

$$f(\lambda) = \pi/\sqrt{\lambda} \quad (9)$$

Where, λ is the elongation ratio.

The maximum tearing energy of each tire rubber material was calculated by using the finite element analysis platform. The maximum tear energy of rubber specimens under cyclic tension of 10 %, 15 %, 20 %, 25 %, and 30 % strain is shown in Fig. 4.

After calculation, transformation Eq. (10) can obtain:

$$dN = da/BT_{\max}^F \quad (10)$$

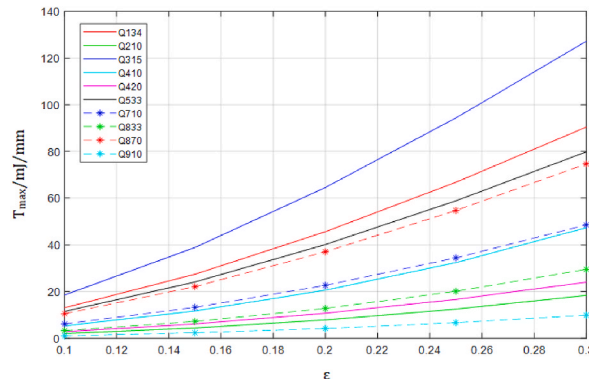


Fig. 4. The maximum tearing energy of the rubber specimen under various strains.

The crack growth rate can be obtained by rubber fatigue tensile test. By analyzing the relationship between the crack propagation rate and maximum tear energy of rubber materials, the fatigue parameters of each material in the Lake Lindley model are fitted using a logarithmic coordinate system curve. The curve is shown in Fig. 5.

By integrating both sides of Eq. (10) at the same time, we can get:

$$N = \int_{l_1}^{l_2} \frac{dl}{BT^F} = \frac{1}{B(1-F) \left(\frac{2E}{n} E_0\right)^F} (l_2^{1-F} - l_1^{1-F}) \tag{11}$$

In Eq. (11), N is the number of cycles when rubber fatigue failure occurs.

Based on the Lake-Lindley fatigue model, this paper uses the finite element software to obtain the maximum tear energy of each rubber material, and uses the rubber fatigue tensile test bench to obtain the crack growth rate of each rubber material at the specified temperature. Finally, the third stage curve of the Lake-Lindley fatigue model is obtained by fitting the maximum tear energy and crack growth rate, and the material constant in the model is obtained to calculate the tire fatigue life. The tire fatigue life analysis results are shown in Fig. 6.

The main reason for tire fatigue failure is that the tire undergoes alternating deformation under load, followed by permanent deformation, causing the molecular chain to slowly break and fail. From force analysis, it can be seen that the stress and strain at the end point of the tire body's reverse envelope and the tire shoulder position are the highest during the loading stage. And through temperature field analysis, it can be known that the tire shoulder is the second highest temperature position. Therefore, the above two positions are dangerous points for fatigue failure.

The values shown in the fatigue life distribution cloud are logarithmic values of life, and the true fatigue life needs to be converted into hours by Eq. (12).

$$T = \frac{10^X \cdot 2\pi R}{V \cdot 10^6} \tag{12}$$

Where T is the tire fatigue life, X is the logarithmic value of the life at the fatigue damage point, R is the rolling radius, and V is the rolling speed.

According to the cloud chart of fatigue life analysis results, it can be seen that the minimum point of fatigue life of the tire is located near the shoulder, the value is 106,111 cycles, and the fatigue damage time can be calculated from Eq. (12) is 146.92 h.

2.2. Experimental validation of thermal fatigue life simulation analysis of tires

The object of this study is 12.00R20 size tire (18-ply grade), and the experimental conditions are set according to the requirements of "GB/T 2977-2016 Truck Tire Specifications, Size, Air Pressure and Load", as shown in Table 6.

In order to verify the accuracy of the tire fatigue analysis results, this paper conducted enhanced endurance experiments on the tire studied in this paper with the help of its laboratory and experimental equipment.

The four-station endurance experiment machine used for the experiment is shown in Fig. 7.

3. Result

In order to verify the accuracy of tire fatigue analysis results, finite element simulation and experiments of four design solutions of this tire were conducted in this paper. The difference between the four schemes is reflected in the height of the down region and the coverage of nylon cloth. The four schemes are shown in the table below.

The comparison results between tire life simulation analysis and experiments are shown in Table 8.

From the comparison results of experiment and simulation, the thermal fatigue life of the tire obtained through simulation calculation is very close to the actual tire fatigue life. The tire finite element model can effectively simulate the real structure of the tire,

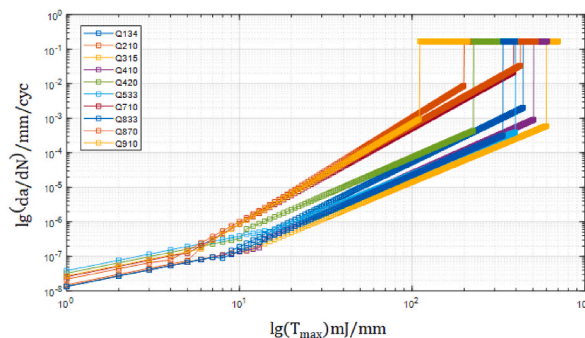


Fig. 5. Fatigue model curve of each rubber in the tire.

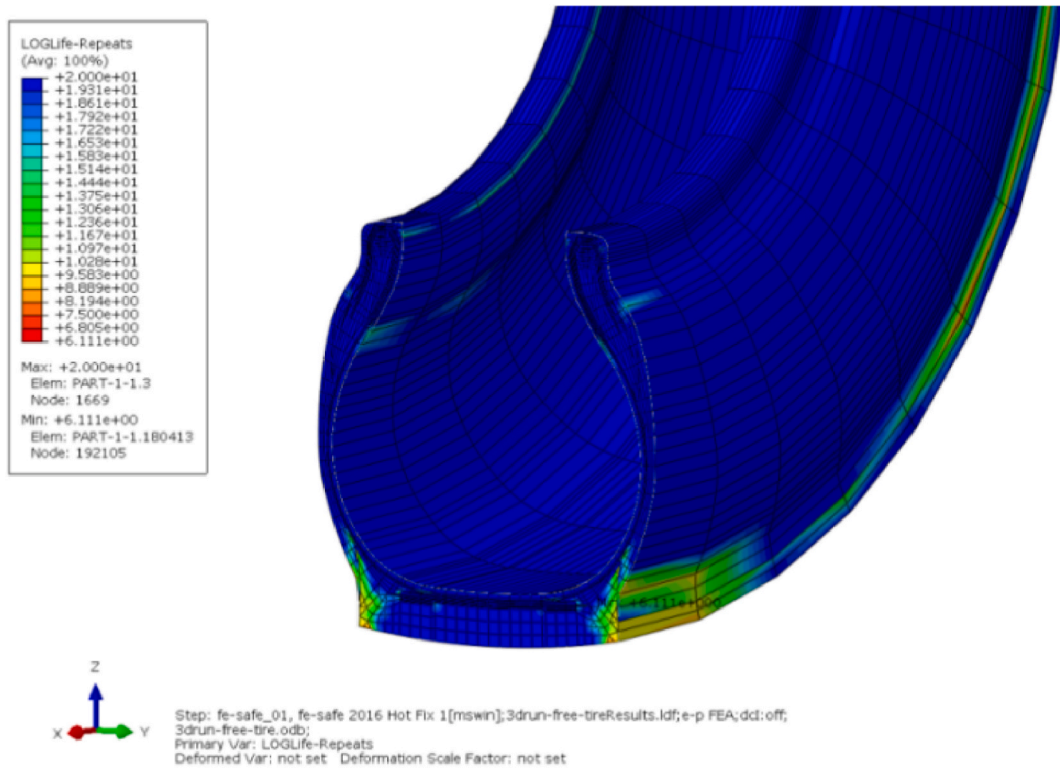


Fig. 6. Tire fatigue life distribution cloud map.

Table 6
Condition parameters of tire reinforcement fatigue endurance test.

Experimental conditions parameters	Specific values
Ambient temperature	25 ± 3 °C
Drum diameter	1707 mm
Drum speed	30 km/h
Drum load	75 kN
Tire internal pressure	0.65 MPa

Table 7
Four tire design schemes.

	Height of the down region (mm)	Coverage of nylon cloth
Scheme 1	90.2	outside
Scheme 2	79.4	outside
Scheme 3	90.2	inside and outside
Scheme 4	90.2	inside and outside, disconnecting in the middle

while the simulation of temperature field takes into account the change of tire rubber fatigue parameters caused by the temperature change, which in turn causes the tire fatigue life changes. The errors shown in the table mainly come from the finite element modeling errors and the errors caused by material experiments and parameter fitting, but these errors are below 10 %, so they basically meet the needs of engineering practice.

4. Optimal design of radial tire section layout

4.1. Tire sensitivity analysis by region

The material properties of rubber materials in tires affect the overall fatigue performance of tires, so it is theoretically possible to achieve the improvement of tire fatigue performance by adjusting the material properties of each rubber in tires. The tire studied in this



Fig. 7. Four-station durability testing machine.

Table 8
Comparison of tire fatigue life simulation and experimental results for four schemes.

	Experimental results (h)	Simulation results (h)	Error
Scheme 1	75	71.14	5.15 %
Scheme 2	50	45.01	9.98 %
Scheme 3	150	146.92	2.05 %
Scheme 4	80	77.74	2.82 %

paper is a radial tire used for heavy-duty vehicles, and it can be seen from its material distribution diagram that different areas are composed of different types of rubber materials, and there are as many as ten kinds, so if all areas are taken into consideration and the material parameters of each area are used as design variables for the establishment and solution of the tire optimization model, it is conceivable that it will be a huge workload. Therefore, before establishing the tire optimization model, it is necessary to conduct the rubber material design sensitivity analysis of each area of the tire and find out the area where the material change has a greater impact on the tire fatigue life performance as the key research object.

Design sensitivity analysis (DSA) is to study the degree of influence of design variables on the objective function, and to filter out the design variables with higher correlation with the objective function and then find out the focus and direction of optimal design. In this paper, the thermal fatigue life of the tire is used as the objective function, and the elastic modulus of the rubber material in each area of the tire is selected as the design variable, and the design sensitivity analysis is conducted for each area of the tire. The material sensitivity results for each region of the tire are shown in Table 9.

As can be seen from the table, the DSA values in the crown, shoulder and belt layer areas are significantly larger than the other areas, i.e. the material changes in these areas have a greater impact on the overall fatigue life of the tire. The reason is not difficult to explain, according to the fatigue life finite element analysis results of the four designs of the tire, the minimum value points in the fatigue life distribution cloud are all located in the tire shoulder, and the area adjacent to the shoulder is the crown and the belt layer, so the tire fatigue life of these three areas of material changes are more sensitive. In addition, according to the previous studies of the group, the fatigue damage of radial tires mainly occurs at the end of the steel wire of the belt layer and the shoulder joint, as well as the end of the carcass backpack [19–21], and the results of the previous fatigue life analysis also confirm this view. Therefore, the next study in this paper will focus on the shoulder, crown and the belt layer area as the key research areas for the tire fatigue life optimization model.

Table 9
Sensitivity of tire fatigue life to materials in each region.

Region	$\hat{\gamma}_{DSA}$	Region	$\hat{\gamma}_{DSA}$
Crown	0.423	Shoulder	0.455
Side	0.042	Bead	0.153
Wear	0.315	Belt	0.402
Down	0.112	Carcass	0.121
Up	0.091	Inner	0.033

4.2. Mathematical model for thermal fatigue life optimization of tires

Establishing a mathematical model of the optimization problem is an effective way to improve the efficiency of the optimization design. For the establishment of the mathematical model of the optimization design problem, it is necessary to first clarify the three elements of the optimization design: objective function, design variables and constraints, and then by solving the optimal solution of the function of the mathematical model of the optimization problem under the constraints, the optimal design solution of the optimization problem in the design space can be determined [22]. The mathematical model function of the optimization design problem is as follows.

Objective function.

$$\min f(X) = f(x_1, x_2, \dots, x_n) \quad (13)$$

Design variables.

$$X = [x_1, x_2, \dots, x_n]^T \quad (14)$$

Constraints.

$$\begin{cases} h_j(X) \leq 0, j=1, 2, \dots, p \\ g_k(X) \leq 0, k=1, 2, \dots, q \\ x_i^{\min} \leq x_i \leq x_i^{\max}, i=1, 2, \dots, n \end{cases} \quad (15)$$

4.2.1. Objective function

This paper aims to improve the thermal fatigue life of the tire, so the tire fatigue life under free rolling conditions considering the influence of temperature field is taken as the objective function of this optimization task, with the maximum tire thermal fatigue life as the optimization objective. Based on the above finite element analysis process of the tire, the analysis and calculation of the tire thermal fatigue life can be done quickly by using the tire finite element analysis platform combined with the fatigue life analysis software Fe-safe.

4.2.2. Design variables

For the optimization design problem, the selection of design variables is very critical. The reasonable selection of design variables can not only improve the computational speed of the optimization problem, but also improve the accuracy of the approximation model of the optimization problem.

The performance of the tire is affected by the tire structure parameters and material parameters together. Based on the results of the previous sensitivity analysis of the rubber material in each area of the tire, the shoulder, crown and belt layer, which have the greatest influence on the tire fatigue life, were selected as the key research objects for the next optimization analysis, so the material parameters of the corresponding rubber material in these three areas were firstly selected as design variables.

In this paper, the Yeoh model is selected as the intrinsic structure model of rubber materials, and the material parameters of rubber materials in this model are mainly C_{10} , and C_{20} , and C_{30} three. C_{10} is half of the initial shear modulus, which determines the small deformation region of the material curve. C_{20} is the softening parameter at deformation, which determines the deformation region in the material curve. C_{30} is the hardening parameter at large stress, which determines the large deformation region of the material curve.

According to the literature, the initial modulus of elasticity of rubber can be calculated by Eq. (16).

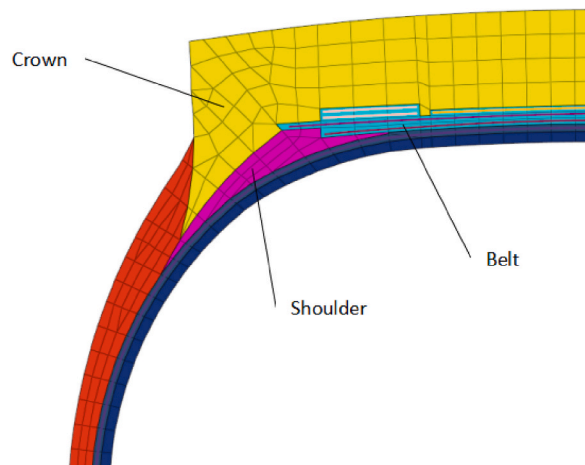


Fig. 8. The position of shoulder, crown and belt rubber on the tire section.

$$E_0 = 6C_{10} \quad (16)$$

It can be seen that the initial modulus of elasticity of rubber is proportional to the parameter C_{10} is proportional. In addition, the deformation range of the tire rubber is generally less than 20 % during the actual operation of the tire, which is located in the small deformation region of the material curve [23]. Therefore, by adjusting the rubber formulation to change its modulus of elasticity, and thus changing the material parameters C_{10} . The fatigue life of the tire can be improved by adjusting the rubber formulation to change its modulus of elasticity and thus the material parameters [4].

For the above reasons, the modulus of elasticity of the rubber materials in the shoulder, crown and belt layer regions were selected as design variables in this paper. The position of the three areas on the tire section is shown in Fig. 8. For the modulus of elasticity of shoulder, crown and belt rubber, the control variable method is used to change the modulus of elasticity of one of the rubber materials, and the modulus of elasticity of the other two rubber materials is kept constant to study the effect of each design variable on the thermal fatigue life of the tire as a function of the target, and for the convenience of analysis, the fatigue life of the tire is temporarily replaced by the logarithmic value X of the fatigue damage point in Eq. (12).

Under the constraint conditions, the modulus of elasticity of shoulder rubber, crown rubber and belt layer were changed to study their effects on the thermal fatigue life of the whole tire, and the relationship curves between the modulus of elasticity of shoulder rubber, crown rubber and belt layer and the thermal fatigue life of the tire are shown in Fig. 9.

In addition, it has been studied that the structure of the belt layer has a large effect on the tire fatigue life, where the angle of the belt cord has a large effect on the strain energy density at the end of the belt layer, which in turn affects the tire fatigue life to a larger extent [24,25]. The position of 1#belt cord and 2#belt cord on the tire section is shown in Fig. 10. The subject of this paper is a radial tire for a heavy vehicle, where the differences in the structure and function of each of its belt layer lead to different effects of their forces on the surrounding rubber material [26,27]. Among them, the 1# belt layer and 2# belt layer as working layers are usually subjected to larger load pressure and therefore exert larger force on the nearby rubber structure, causing them to produce larger stress concentrations leading to fatigue damage. It can be seen that 1#belt layer and 2#belt layer have a greater influence on the fatigue life of the whole tire, so this paper takes the tire 1#belt cord and 2#belt cord angle also as the tire thermal fatigue life optimization design variables, and also adopts the control variable method to study their influence on the tire thermal fatigue life.

Under the constraint condition, change the angle of 1# and 2# belt cord to study its effect on the thermal fatigue life of the whole tire, and plot the relationship curve between 1# and 2# belt cord angle and tire thermal fatigue life, as shown in Fig. 11.

Based on the above analysis, this paper finally selects five parameters as the design variables, namely, the modulus of elasticity of shoulder rubber, the modulus of elasticity of crown rubber, the modulus of elasticity of belt rubber, the angle of 1# belt cord and the angle of 2# belt cord, for the construction of the tire thermal fatigue life optimization model.

4.2.3. Constraints

The design variables of the optimization model were determined based on the actual tire manufacturing process realization provided by the tire plant as shown in Table 10.

4.3. Optimizing the approximate model

The approximate model is a functional relationship between the input and output quantities obtained by fitting the relevant mathematical approximation methods, and the approximate model method is often used to solve the relevant optimization design problems. In some computationally intensive simulation and optimization problems, the use of approximate models instead of finite element models can reduce the number of simulation program calls and can improve the optimization efficiency by orders of magnitude.

After comparing the fitting accuracy of different approximation models, this paper finally selects the response surface model to fit

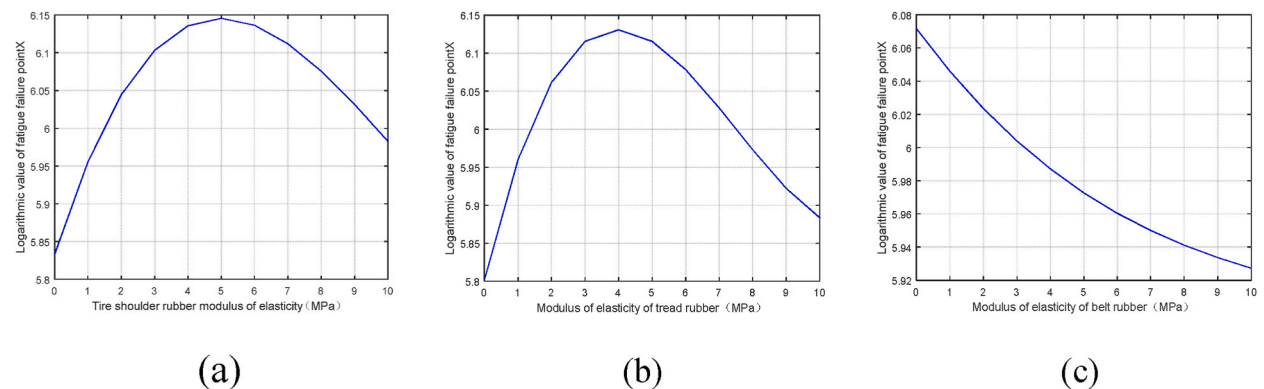


Fig. 9. Relationship between elastic modulus of different parts and tire thermal fatigue life:(a)tire shoulder rubber; (b)tire crown rubber; (c)tire belt rubber.

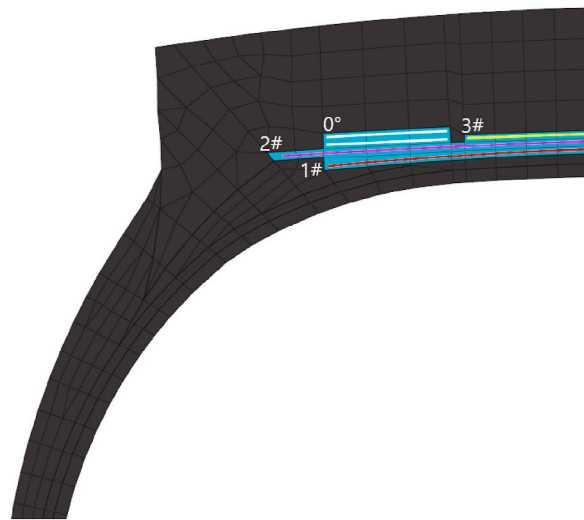


Fig. 10. The position of shoulder, crown and belt rubber on the tire section.

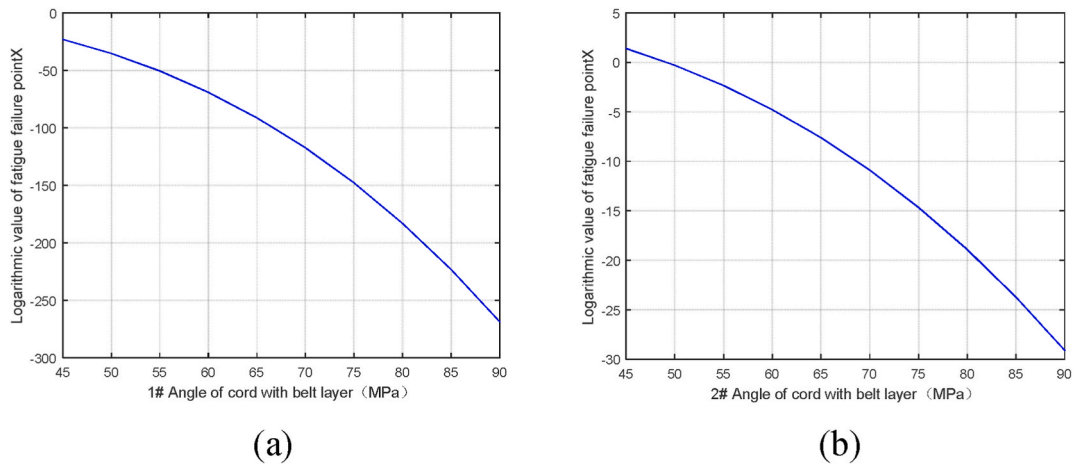


Fig. 11. Relationship between 1#, 2#belt cord angle and tire thermal fatigue life:(a) 1#belt cord; (b) 2#belt cord.

Table 10
Range of values of experimental design variables.

Name	Code Name	Initial Value	Range of values
Tire shoulder rubber modulus of elasticity	x_1	3.0 MPa	0~10 MPa
Modulus of elasticity of tread rubber	x_2	3.41 MPa	0~10 MPa
Modulus of elasticity of belt rubber	x_3	0.73 MPa	0~10 MPa
1# Angle of cord with belt layer	x_4	66°	45~90°
2# Angle of cord with belt layer	x_5	75°	45~90°

the approximation model and obtains the response surface function of tire thermal fatigue life, and will use this function instead of finite element simulation analysis for the next optimization.

Response surface model (RSM) is a regression model that fits the relationship between input and output functions by polynomials [28]. Its advantages are simple function construction, small computational effort, fast convergence, and good fitting effect in the case of few design variables, while its function polynomial coefficients can reflect the degree of influence of design variables on the response target. The response surface model is a regression approximation model, and the regression approximation model has a better noise filtering effect for the finite element simulation problem which has certain model errors.

For the thermal fatigue optimization problem of radial tires studied in this paper, the second-order response surface model is chosen here to express the relationship between the design variables and the response. The second-order response surface model basis function

is expressed as

$$1, x_1, x_2, \dots, x_n, x_1^2, x_1x_2, \dots, x_1x_n, \dots, x_n^2 \tag{17}$$

The second-order response surface function is given by

$$y = r_0 + \sum_{j=1}^n r_j x_j + \sum_{j=n+1}^{2n} r_j x_{j-n}^2 + \sum_{i=1}^{n-1} \sum_{j=i+1}^n r_{ij} x_i x_j \tag{18}$$

Where n is the total number of design variables, and x_i is the first i is the first design variable, and r_0 is the constant term.

The relationship between the number of basis functions N and the number of design variables n The following relationship exists between:

$$N = 1 + C_n^1 + C_n^2 = \frac{(n+1) \times (n+2)}{2 \times 1} \tag{19}$$

4.4. Optimal Latin hypercube experimental design

The design variables are shoulder rubber modulus of elasticity, tread rubber modulus of elasticity, belt rubber modulus of elasticity, 1# belt cord angle and 2# belt cord angle, and the tire thermal fatigue life performance under free-rolling condition is used as the evaluation index, and optimal Latin hypercube sampling is used for the experimental design. The approximate model established in this paper contains five design variables, so the test design needs to collect at least $(5+2) \times (5+1)/2 = 21$ sample points. 30 sample points are collected in this paper to generate the design matrix, and the tire thermal fatigue life is calculated by using the tire FEA software, and the results are shown in Table 11.

4.5. Response surface modeling

In this paper, we choose the second-order response surface approximation model, combine the test design scheme data in Table 11, use the least squares method to fit the response surface function to the tire thermal fatigue life, get the coefficients of each basis function in the response function, and get the function expression of the second-order response surface approximation model of tire thermal fatigue life (20).

Table 11
Test design scheme and fatigue life results.

	Modulus of elasticity of shoulder rubber	Modulus of elasticity of crown rubber	Modulus of elasticity of belt rubber	2# Angle of cord with belt (°)	2# Angle of cord with belt (°)	Thermal fatigue life (h)
1	1.408	1.627	4.579	84.761	44.725	108.762
2	0.103	3.697	6.360	54.484	40.595	100.776
3	7.545	7.951	4.217	8.120	68.469	149.261
4	5.738	1.035	7.391	22.820	26.213	129.385
5	5.481	6.988	8.271	52.691	76.458	153.662
6	5.089	7.141	7.950	65.588	17.987	133.332
7	9.6891	0.972	2.036	49.288	55.600	140.367
8	8.401	5.236	9.287	74.681	65.815	150.642
9	0.376	9.647	1.592	47.208	49.017	99.753
10	0.924	6.545	9.867	18.291	38.470	91.776
11	1.671	9.189	5.573	75.917	52.560	103.258
12	3.476	2.323	2.919	28.230	19.508	125.764
13	3.155	3.595	7.093	89.546	84.813	145.167
14	3.683	2.366	9.599	83.090	27.779	136.295
15	6.476	9.823	2.603	30.706	7.281	151.981
16	2.954	0.182	6.963	57.866	31.675	99.762
17	4.111	4.170	5.115	67.893	0.176	136.726
18	1.088	1.938	8.890	3.678	23.491	108.359
19	9.231	4.782	3.705	10.455	69.173	121.845
20	4.394	7.337	3.505	14.563	13.791	138.976
21	7.710	5.833	3.128	2.373	72.315	167.798
22	6.868	5.425	1.150	69.784	58.825	181.438
23	8.270	8.532	4.819	16.001	4.129	136.124
24	7.001	3.163	0.240	38.823	11.835	140.159
25	4.938	0.527	0.792	25.959	35.151	132.151
26	9.510	8.711	8.597	35.293	82.548	136.742
27	2.292	2.966	0.581	60.975	79.749	141.747
28	3.007	3.411	0.724	66.004	75.719	145.457
29	6.197	8.012	1.738	80.728	47.552	152.174
30	8.680	4.517	6.173	40.920	61.185	159.636

$$\begin{aligned}
 L(x_i) = & -65.972 + 71.615x_1 - 1.659x_2 + 22.288x_3 - 1.003x_4 - 1.134x_5 - 0.255x_1x_2 \\
 & - 1.737x_1x_3 + 0.196x_1x_4 - 0.148x_1x_5 - 0.82x_2x_3 + 0.253x_2x_4 + 0.194x_2x_5 \\
 & + 0.237x_3x_4 - 0.35x_3x_5 + 0.015x_4x_5 - 5.295x_1^2 - 0.653x_2^2 + 0.128x_3^2 - 0.04x_4^2 \\
 & + 0.034x_5^2
 \end{aligned}
 \tag{20}$$

The accuracy of the approximate model affects the reliability of the subsequent optimization design scheme. Therefore, after completing the fitting of the response surface model, it is necessary to test its model accuracy. Calculate the error analysis parameters of the tire thermal fatigue life response surface model, and the specific results are shown in Tables 12 and 13.

From Tables 12 and 13, it can be seen that the complex correlation coefficient and corrected complex relationship values of the tire thermal fatigue life response surface model are both greater than 0.85. In addition, the response surface model of tire thermal fatigue life is subject to F-test, check the F-test table when the significance level $\alpha = 1$, the F-test table showed that it met:

$$F = 13.7449 > F_{0.01}(20, 16) = 3.26
 \tag{21}$$

The F-test shows that the response surface model of tire thermal fatigue life is significant, and the model has high accuracy, so it can be used in the subsequent optimization design analysis.

4.6. Optimized design for thermal fatigue life of radial tires

This section is based on the model to optimize the design of the elastic modulus of the three rubber materials and the angle of belt cord, and then improve the thermal fatigue life performance of the tire.

The optimal design model for the thermal fatigue life of a tire can be expressed as

$$\begin{cases} \max L(x_i) \\ x_i^{\min} \leq x_i \leq x_i^{\max} (i = 1 \sim 5) \end{cases}
 \tag{22}$$

Where, $L(x_i)$ is the tire thermal fatigue life; x_i is each design variable, and x_i^{\max} and x_i^{\min} are the upper and lower limits of each variable.

Based on the initial values and constraints of the model variables mentioned above, the genetic algorithm is used to optimize the response surface model, and the parameters of the genetic algorithm are set as follows: the population size is 50 and the number of genetic generations is 35. The results of the optimized design solution for the thermal fatigue life of the tire compared with the original solution are shown in Table 14.

4.7. Simulation verification of optimized design solutions

In order to verify the accuracy and credibility of the optimized design, finite element simulations were performed for the above optimized design scheme, and the error was calculated by comparing the calculation results of the approximate model with results of the finite element simulation. According to the values of the design variables of the optimized design scheme, the thermal fatigue life of the tire is calculated by using the FEA software, and the calculation results are shown in Fig. 12.

It can be seen that the minimum value of the tire fatigue life cloud after the optimized design is still located at the shoulder, the fatigue wear point is located at the shoulder, and its value is 6.201.

The simulation verification and error analysis of the tire fatigue life response surface model shows that the model has high fitting accuracy and can replace the finite element simulation analysis program to complete the rapid calculation of tire fatigue life.

5. Discussion

The error between the approximate model calculation results and the finite element simulation calculation results is only 3.6 %, which indicates that the response surface model of tire thermal fatigue life has high accuracy and reliability, and can be used for the prediction of tire thermal fatigue life as well as the optimization work. Compared with the original design, the optimized design improves the tire fatigue life by about 25 %, which achieves the expected purpose better.

6. Conclusions

In this study, tire thermal fatigue life simulation is carried out by finite element platform, and the accuracy of the simulation model is verified through experiments, and the response surface approximation model method combined with genetic algorithm is used to

Table 12
Complex correlation coefficient and modified complex correlation coefficient of tire thermal fatigue life response surface model.

Response surface modeling	R^2	R_{adj}^2
Tire thermal fatigue life	0.945	0.876

Table 13
Error analysis table of tire thermal fatigue life response surface model.

Error source	Sum of squared fluctuations	Freedom f	Mean square V	Variance F
Fitting error S_n	19.9816	20	0.9991	13.7449
Residual error S_c	1.1630	16	0.0727	
Comprehensive error S_n	21.1446	36		

Table 14
Comparison between the optimized design scheme of tire thermal fatigue life and the original scheme.

Programs	Modulus of elasticity of shoulder rubber	Modulus of elasticity of crown rubber	Modulus of elasticity of belt rubber	2# Angle of cord with belt (°)	2# Angle of cord with belt (°)	Thermal fatigue life (h)
Original design	3.0	3.41	0.73	66	75	146.921
Optimized design	6.13	5.36	2.42	75.26	64.75	187.276

Table 15
Comparison of approximate model and finite element simulation calculation results.

	Approximate model calculation results	Finite element simulation results	Error
Tire thermal fatigue life (h)	187.276	180.752	3.6 %

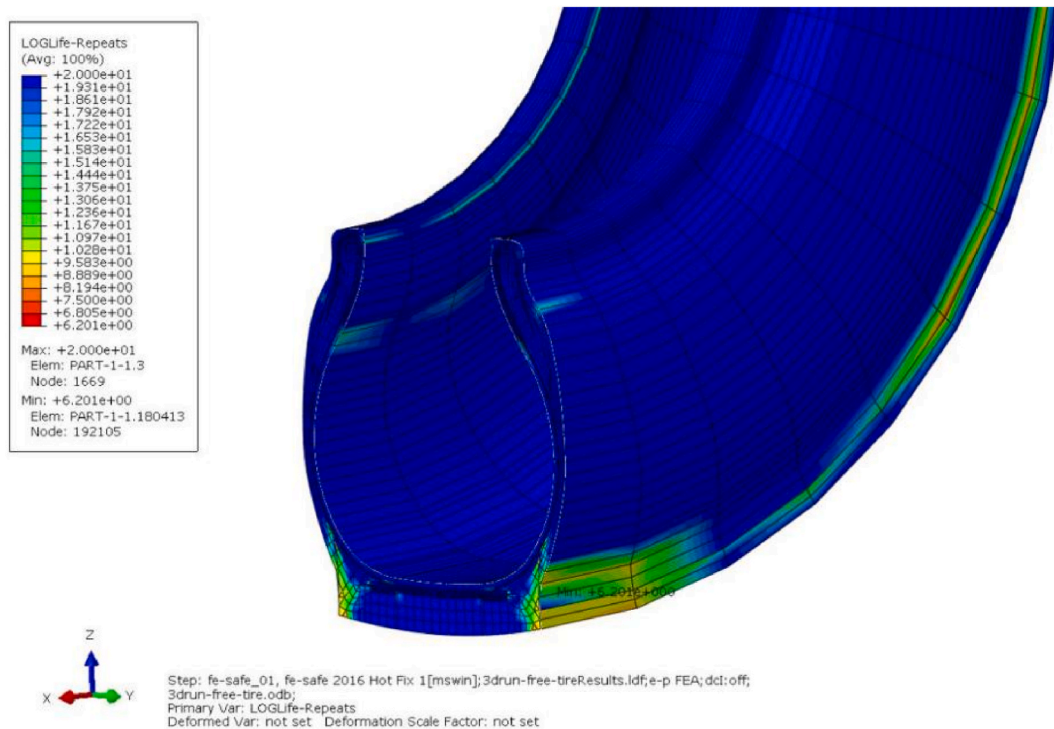


Fig. 12. Fatigue life cloud diagram of the optimized design scheme.

achieve the optimal design of tire thermal fatigue life. Firstly, the sensitivity analysis of rubber material in each area of the tire is conducted to find out the area where the material change has a greater impact on the tire fatigue life performance as the key research object; then, the three elements of the tire fatigue life optimization design problem are determined according to the results of the area sensitivity analysis and the actual situation of tire manufacturing process realization, and the tire thermal fatigue life optimization model is established; then the optimal Latin hypercube sampling is used to The response surface model with high accuracy was established by using the response surface method combined with the experimental design data, and the response surface model was optimized by using the genetic algorithm, and then the optimized design scheme of tire thermal fatigue life was obtained; finally, the reliability of the optimized design scheme was verified by the simulation analysis of the optimized tire, and compared with the original

design scheme, the tire fatigue life of the optimized design is improved by about 25 %.

Declaration of competing interest

The authors declare that they have no known competing financial interests or personal relationships that could have appeared to influence the work reported in this paper.

Acknowledgments

Funding from the National Natural Science Foundation of China(Grant No. 51475255) is gratefully acknowledged.

References

- [1] Liangqing Ma, Yan Wang, Ning Sun, Ji Tao, Huiyun Jiao, Current situation and development of China's automobile tire industry, *Tire Industry* 29 (12) (2009) 707–715.
- [2] Yu Qi, Jianping Ding, Overview of the development of skeleton materials for all-wire radial tires, *Rubber Technology Market* (16) (2004) 12–13.
- [3] Minglei Jiang, Fatigue Life Simulation Study of All-Steel Radial Tires, Master's Thesis, South China University of Technology, 2016.
- [4] G.-L. Wang, B. Lin, D.-F. An, S.-C. Ying, Fatigue performance optimization of radial tires based on sensitivity analysis, *Automot. Eng.* (4) (2008) 354–356.
- [5] Jiaojiao Yang, Jianhao Zhang, Yongfeng Zhang, Optimization of tire bead durability performance based on finite element analysis, *Rubber Science and Technology* 19 (3) (2021) 114–116.
- [6] Jialei Ye, Hongyan Wang, Haiyan Zhang, Fei Wu, Xiaoping Qiu, Zhiquan Wang, Optimization of low-profile radial tire belt bundle ply structure, *Tire Industry* 38 (7) (2018) 399–400.
- [7] Yong Zhang, Optimization Design Method of Vehicle Lightweight Based on Approximate Model, Doctoral Dissertation of, Hunan University, 2009.
- [8] J.P.C. Kleijnen, *Statistical Tools for Simulation Practitioners*, marcel Dekker, new York, 1987.
- [9] D. Lee, J. Kim, S. Kim, K.-H. Lee, Shape design of a tire contour based on approximation model, *J. Mech. Sci. Technol.* 25 (2011) 149–155.
- [10] Debiao Meng, Shunqi Yang, Yu Zhang, Shun-Peng Zhu, Structural reliability analysis and uncertainties-based collaborative design and optimization of turbine blades using surrogate model, *Fatig. Fract. Eng. Mater. Struct.* 42 (6) (2019) 1219–1227.
- [11] Y.Q. Li, Research and Optimization Design of Tire Crown Parameters on Tire Grip and Durability Performance, Master's thesis, Shandong University of Technology, 2021.
- [12] Zehao Su, Li Jia, Yong Zhanfu, Qingchun Wang, Finite element analysis of tire life based on steady-state temperature field, *Tire industry* 38 (12) (2018) 711–718.
- [13] Zehao Su, Improved Design of Tire Structure Based on Thermal Fatigue Life Theory, Master's thesis of, Beijing Forestry University, 2020.
- [14] A. Shida, Rolling resistance simulation of tire using static finite element analysis, *Tire Sci. Technol.* 2 (27) (1999) 84–105.
- [15] A.G. Thomas, et al., The development of fracture mechanics for elastomers, *Rubber Chem. Technol.* 67 (1994) 50–60.
- [16] Wenbin Shangguan, Xiaoli Wang, Xiaocheng Duan, Guobing Liu, Jiao Yan, Experimental and modeling methods for crack propagation in rubber materials of vibration isolators under variable amplitude loading, *J. Mech. Eng.* 15 (8) (2015) 50–58.
- [17] G.J. Lake, B.E. Clapson, Truck tire groove cracking theory and practice, *Rubber Chem. Technol.* 44 (5) (1971) 1186–1202.
- [18] G.J. Lake, Fatigue and fracture of elastomers, *Rubber Chem. Technol.* 3 (68) (1995) 435–459.
- [19] Yong Zhanfu, Preparation and Fatigue Fracture Mechanism of Magnetorheological Elastomer, Doctoral Dissertation of, Qingdao University of Science and Technology, 2018.
- [20] Yimeng Xie, Durability Analysis of a Radial Tire Based on Finite Element Method, Master's thesis of, Beijing Forestry University, 2017.
- [21] Li Jia, Yong Zhanfu, Qingchun Wang, Yimeng Xie, Design of rubber material fatigue testing machine and establishment of fatigue life model, *Rubber technology* 8 (3) (2018) 12–18.
- [22] Bingxin Zhang, Optimization Design of Stirred Immersion Tank Based on Response Surface Method, Master's thesis from, Jilin University two thousand and twenty-one, 2018.
- [23] Yunpeng Shi, Research on Technology and Application of Combined Approximation Model Based on Radial Basis Function, Master's thesis of, Xi'an University of Technology, 2021.
- [24] Jianwei Zhou, Bead Sensitivity Analysis of Radial Tire Based on Combination Model Technology, Master's thesis of, China University of Science and Technology, 2010.
- [25] N. Koronovic, Performance evaluation of cord material models applied to structural analysis of tires, *Compos. Struct.* 224 (2019), 111006.
- [26] Baokai Wang, Structural Design, Belt Layer Optimization and Performance Study of 205/55R16 Radial Tire, Master's thesis of, Qingdao University of Science and Technology, 2020.
- [27] Judong Zhang, Zejun Wang, Ying Zhang, Shaozhi Shan, Fuzhong Zhang, Finite element analysis of the influence of belt angle on the performance of all-steel radial truck tire, *Tire Industry* 38 (8) (2018) 472–474.
- [28] Wei Yan, Research on Optimization of Cooling Performance of Microchannel of Cold Plate Based on Response Surface Method, Master's degree thesis of, Jilin University, 2020.